RESEARCH ARTICLE

Macromolecular Symposia

www.ms-journal.de

Alginate Blocks and Block Polysaccharides: A Review

*Amalie Solberg, Kurt I. Draget, Christophe Schatz, and Bjørn E. Christensen**

Alginates consist of distinct blocks with different physical properties. This short review focuses on research carried out in Trondheim related to the early discovery of the block structure, their isolation, their different chemical and physical properties, and how they recently are utilized in diblock polysaccharides to obtain new nanostructuring properties.

1. Alginate Structure

Alginates are naturally occurring block polysaccharides found in brown seaweeds and produced by some bacteria. In seaweeds alginates equilibrate with sea water cations, especially Ca^{2+}, to form Ca-alginate gels which contribute to strength and elasticity of the plant tissues. The presence in alginates of the three principal block types (**Figure 1**) is a result of an enzymatic processes involving mannuronan-C5-epimerases.[1] These enzymes work on the homopolymeric mannuronan, converting at the polymer level in-chain 4-linked β-D-mannuronate (M) to its 5-epimer, 4-linked α-L-guluronate (G). The enzymes govern both the extent of epimerization and the distribution of blocks in alginates, which depends on the biological source, growth conditions, and even the type of plant tissue.[2] Pure mannuronan, normally serving as an intermediate, is not found in nature but can be obtained from epimerase-negative mutants of alginate-producing bacteria.

2. Isolation and Characterization of Pure Blocks

The understanding of the modular or block-wise structure of alginates preceded the discovery of epimerases and was long thought to be a result of a complex, sequence-dependent polymerization process, and the distribution of monomers can indeed to some extent be explained by a second order Markov model.[3] Although later being rejected as the key mechanism determining the block structures, the presence of distinct blocks was elegantly proven by studying the fragmentation of alginates by relatively mild acid hydrolysis combined with fractional precipitation of alginic acid. An overview is given in **Figure 2**.

A. Solberg, K. I. Draget, B. E. Christensen
NOBIPOL – Department of Biotechnology and Food Science
NTNU-Norwegian University of Science and Technology
Sem Saelands veg 6/8, Trondheim N-7491, Norway
E-mail: bjorn.e.christensen@ntnu.no
C. Schatz
University of Bordeaux, CNRS
Bordeaux INP, LCPO, UMR 5629, Pessac F-33600, France

The ORCID identification number(s) for the author(s) of this article can be found under https://doi.org/10.1002/masy.202200072

DOI: 10.1002/masy.202200072

These findings also provide the key to methods for the excision of different block types. First, different glycosidic linkages in alginates hydrolyze at different rates when pH is near pK_a of the uronic acids.[8,9] This is ascribed to the participation of the protonated carboxylic acids to intramolecular catalysis.[9,10] The conditions favor the hydrolysis of the G–M linkage, which hydrolyses about one order of magnitude faster that the M–G linkage.[8] As expected, the ratio decreased at higher pH when the carboxylic acids became deprotonated. On the other hand, the G–G linkages hydrolyze slower that the other linkage types, being in some way "protected" by being insoluble below pH 3.2. Secondly, the solubility at low pH, that is, of the acidic forms, is very different for the three block types (Figure 2c). G-blocks precipitate below pH 3.2 where other block types remain water-soluble. Together these observations (summarized in Figure 2a) clearly demonstrated the block-wise structure of alginates as well as providing methodologies to prepare the different block types. For the latter several improvements have later taken place. Pure M-blocks are easily obtainable from pure mannuronan by partial hydrolysis and, analogously to G-blocks (Figure 2b), chromatographic separation according to DP.[6] G-blocks with high purity can be obtained from several seaweed alginates using a modification[4] of the hydrolysis/solubility method in Figure 2a. Alternatively, in vitro epimerization in combination with specific lyases can provide almost any block type.[11]

The purity, composition, and chain length distribution of the block fractions in Figure 2a may vary depending on both the type of alginate and the isolation process. More detailed information is obtained by separation of individual DP as shown in Figure 2b. ^{1}H-NMR spectra provide the content and distribution of M and G residues as well as DP.[11] HPAED-PAD analysis of alginate fractions has been shown to be particularly useful due to its very high resolution.[6,11] **Figure 3** shows an example demonstrating the changes in chain length distribution of the G-block fraction during weak acid hydrolysis.

3. Properties and Roles of the Alginate Blocks

The presence of G-blocks in alginates is intimately linked to their ability to form hydrogels with calcium ions. In brown algae the Ca-alginate (in equilibrium with sea water) provides both mechanical strength and elasticity. Extraction of water-soluble Na-alginate consequently involves calcium removal, predominantly by exchanging Ca^{++} with acid, leading to insoluble alginic acid, followed by neutralization using NaOH, $NaHCO_3$, or Na_2CO_3. Alternatively, calcium chelators can be used to remove calcium ions.

The interaction of alginate blocks with Ca^{++} has been widely studied. This also includes studies on Sr^{++} and Ba^{++} because

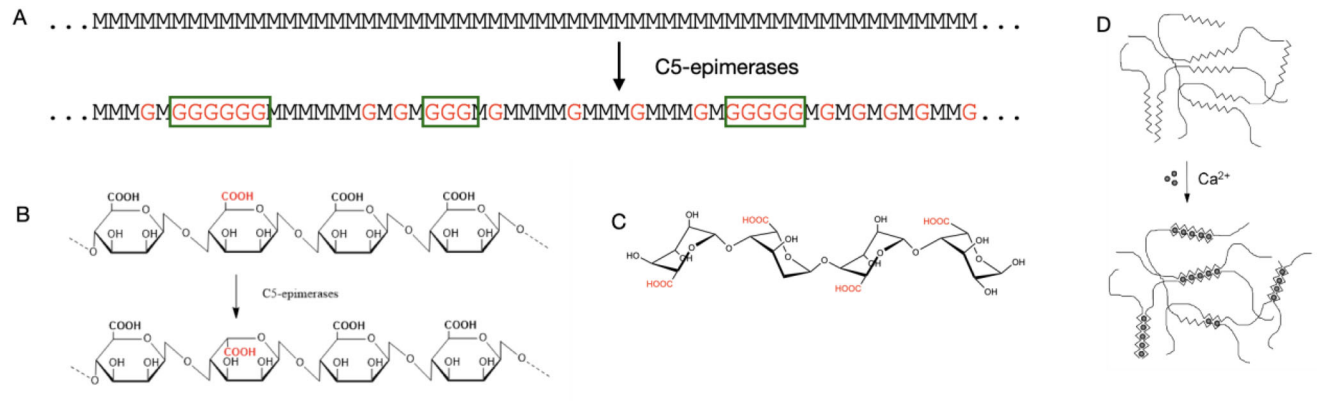

Figure 1. Algal and bacterial alginates are obtained via the intermediate homopolymeric mannuronan (a) by the action of mannuronan C-5 epimerases, converting 4-linked-d-mannuronate (M) to l-guluronate (G) at the polymer level. Haworth formulae are given in (b). The resulting alginates have a blocky structure whose structure depends on the action of several epimerases. G-blocks are depicted in (a) by boxes. The epimerization changes the chair conformations from 4C1 to 1C4. G-blocks thus adopt a "zig-zag" like helical structure with cavities or sites which is the basis for binding of Ca^{++} with high selectivity (c). Calcium binding is associated with chain dimerization leading to the famous egg-box structure for junction zones in calcium alginate gels (d).

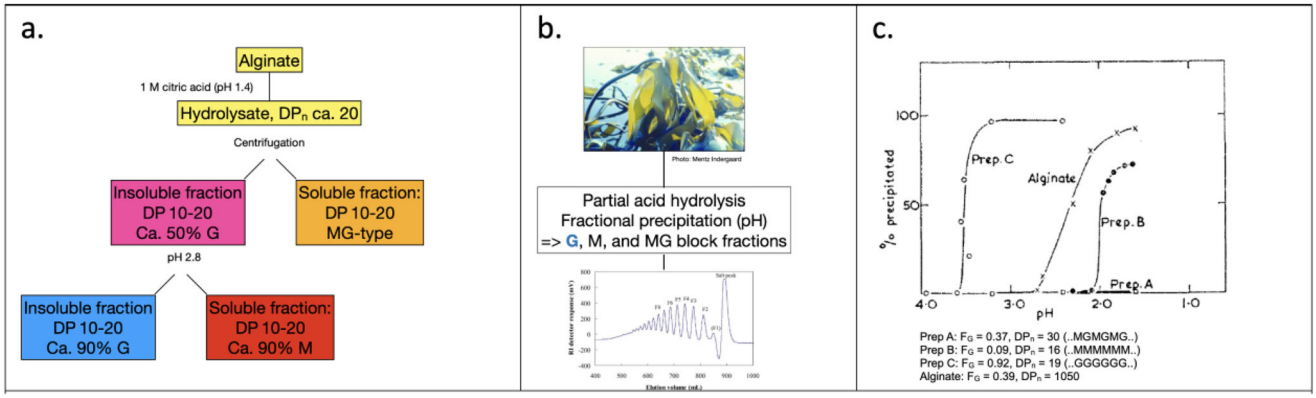

Figure 2. a) Partial acid hydrolysis of alginate to DP_n ca. 20 provides a heterogeneous hydrolysate. The soluble fraction (at pH 1.4) consists predominantly of MG-blocks. The insoluble fraction can, by elevating pH to 2.8, be separated in a soluble fraction (predominantly M-blocks) and a residual insoluble fraction being predominantly G-blocks. The process has later been improved to provide very pure G-blocks.[4] b) Blocks with narrow size distributions are generally obtained by size-exclusion chromatography.[5,6] c) The pH dependence of block solubility. Reproduced with permission.[7] Copyright 1968, Royal Chemical Society.

alginates tend to bind them strongly and selectively concentrate them (by exchange with Ca^{++}). Although practical work with alginate mostly starts with the Na^+ form, studies of the selectivity for divalent cations use Mg^{++} as reference cation because it has the same charge as Ca^{++} and because the strongly hydrated Mg^{++} ions (like Na^+ and other monovalent cations) do not induce gelation or precipitation. Interactions with a divalent cation (Me^{++}) are often expressed[1] through the selectivity coefficient K^{Me}_{Mg} with Mg^{++} as a reference ion:

$$K^{Me}_{Mg} = \frac{X_{Me}}{X_{Mg}} \frac{[Mg^{++}]}{[Me^{++}]} \quad (1)$$

where X refers to the mole fractions of bound cation, whereas $[Mg^{++}]$ and $[Me^{++}]$ are the molar concentrations of cations in solution (at equilibrium). Studies[1] related to cation selectivity resulted in many important findings:

(a) G-blocks bind Ca^{++} only moderately strong if prevented from subsequent aggregation (e.g., using an agarose gel).[13]

(b) G-blocks precipitate with Ca^{++} but the crystal structure has been challenging to study by X-ray crystallography.[14]

(c) In alginates containing G-blocks the Ca/Mg selectivity increases with increasing X_{Ca} reaching a maximum around $X_{Ca} = 0.4–0.5$ before decreasing toward $X_{Ca} = 1$.[1]

(d) The Ca-binding in alginates containing G-blocks shows strong hysteresis: after preparing fully saturated Ca-alginate ($X_{Ca} = 1$) the Ca/Mg-selectivity increases when lowering X_{Ca} and can react values close to 100.[1]

(e) Alginates lacking longer G-blocks, that is, mannuronan or polyalternating (..MGMG.. type) alginate have low Ca-selectivities, typically in the range 2–3.[1]

These, as well as other considerations, have led to the famous "egg-box model" for initial dimerization of alginate G-blocks

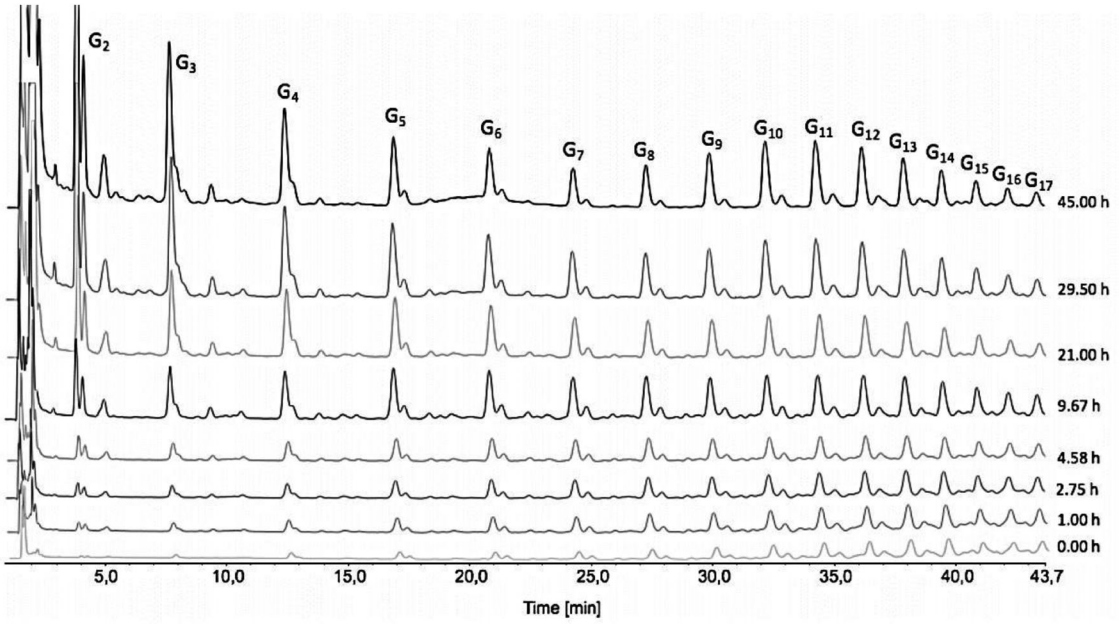

Figure 3. HPAEC-PAD chromatograms demonstrating the formation and distribution of guluronate oligomers during acid hydrolysis (95 °C, pH 3.62). Minor unannotated peaks are ascribed to oligomers containing M residues. Reproduced from ref.[12] Copyright 2022, Royal Society of Chemistry.

with Ca^{++} (schematically illustrated Figure 1d). Although first proposed[15] in 1973 it seems still to be the preferred model.[14,16] However, the dimeric state seems to be unstable and is followed by further growth, leading to large multi-chain junction zones in gels,[17] and precipitation for isolated G-blocks.[12]

4. G-Blocks as Gelation Modifiers

The addition of G-blocks (DP_n in the range 20) during gelation of high molecular weight alginates has demonstrated complex interactions influencing both kinetics and equilibrium modulus, as well as degree of syneresis in the resulting gels.[18,19] In other words, by exploiting the ion binding properties of low molecular weight G-blocks it has become possible to de-couple modification of alginate gel properties from viscosity changes. The presence of G-blocks always slows down the gelling kinetics of high molecular weight alginates and reduces syneresis. The apparent equilibrium modulus in the presence of G-blocks depends on the level of gelling ions present: at low Ca saturation the modulus will be reduced due to competitive ion binding, whereas at high Ca saturation the modulus will become higher than for the high molecular weight alginate alone. The latter is believed to result from G-block being able to interact with and connect topologically restricted G sequences within the high molecular weight alginate, thereby on average shortening the elastic segments. This is a reasonable approach as other studies have shown cross sectional dimensions of alginate gel junctions way above that for dimerization at high Ca saturation.[17]

5. G-Blocks–Mucus Interactions

A rather surprising effect of G-blocks involves the ability to modify other ordered and complex biopolymer systems such as mucus,[20,21] both in the pathological as well as in the nonpathological state. In the first instance, G-blocks have been shown to modulate and normalize abnormally viscous mucus as found in, for example, subjects suffering from cystic fibrosis. G-blocks are possibly able to disrupt complex mucus interactions through electrostatic interactions, although the exact mechanism remains unclear, resulting in a lower cross-linking density and increased mucus mobility. In the second instance, it has been shown that guluronate oligomers are able to modify nonpathological mucus in terms of an overall altering of mucus network architecture (e.g., increased pore size) leading to a reduction in barrier function as reflected in an improved nanoparticle mobility and uptake in such systems. Hence, G-blocks may have a potential in mucosal delivery of nanomedicines. Under any circumstance there is no evidence that G-blocks function as a true mucolytic by depolymerizing mucins but rather to modify mucus architecture by blocking macromolecular interactions.

Taken together, G-blocks present a unique system based on abundant biomass that have important biological and technological properties. When part of alginates they explain, among other, the Ca^{++} binding and gelation, making alginates attractive in biotechnology and biomedicine. However, other possibilities now emerge in the form of engineered block polysaccharides. This is described in the following section.

6. Terminal Versus Lateral Substitution: Block Architectures

Lateral structural modifications (Figure 4a), presently comprising almost all polysaccharide derivatives, generally leads to pronounced changes in physical properties. Lateral decoration of alginates by, for example, peptides or sulfate would, depending on the degree or pattern of substitution, gradually mask the unsubstituted regions necessary for Ca-induced egg-box formation

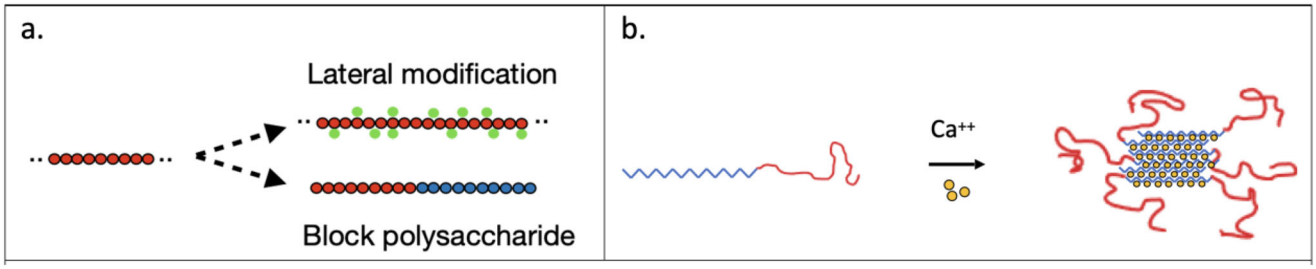

Figure 4. a) Terminal versus lateral substation. b) Ca^{++}-induced self-assembly of a G_m-*b*-Dex_n diblock to form a core-corona nanoparticle. (a) is drawn with permission from ref.[22] Copyright 2022, Elsevier.

or reduce the availability for alginate degrading enzymes. In contrast, terminal conjugation to a second chain would provide a diblock polysaccharide with laterally unsubstituted chains (Figure 4a). Conjugating a Ca-sensitive G-block to a second Ca-insensitive, but water-soluble, block should, according to the principles of synthetic block polymers, provide a system that could in the presence of Ca^{++} self-assemble into a nanoparticle with a Ca-alginate core and an outer corona consisting of the second block (Figure 4b).

7. Engineered Block Polysaccharides

Initial work has focused on G-blocks (G_m, m = DP) terminally coupled to dextran (Dex_n, n = DP) using PDHA (*O,O′*-1,3-propanediylbishydroxylamine) as the linker.[12,22] Dextrans are neutral (uncharged) polysaccharides with a flexible glucan backbone due to the α-1,6-linkages. They may also contain some branches. Dextrans of suitable DP were obtained by partial hydrolysis to cover the DP-range 10–200. The mixture was coupled at the reducing end to PDHA by reductive amination before the PDHA-activated dextrans were separated according to DP by SEC analogous to that shown in Figure 2b. Selected PDHA-activated dextran fractions were subsequently conjugated to G-block fractions of the desired DP, again using reductive amination at the reducing end. G_m-*b*-Dex_n diblocks (fully conjugated PDHA-dextrans) were purified from unreacted G-blocks by semi-preparative SEC. Structures and chain lengths were confirmed by NMR and SEC-MALLS, respectively. As an alternative to PDHA-dextran G-blocks were terminally connected to oxyamine-PEG to obtain the G_m-*b*-PEG_n diblock using a related protocol. The chemistry and kinetics of reactions of oligo- and polysaccharides with dioxyamines (PDHA) and dihydrazides was recently reviewed.[22]

Self-assembly of the diblocks G_{11}-*b*-Dex_{100} and G_{40}-*b*-Dex_{100} with Ca^{++} was studied[12] by dynamic light scattering using a dialysis setup with a nominal membrane cut-off of 100–500 Da. Pure G-blocks led to precipitation, whereas the diblocks did not. For G_{40}-*b*-Dex_{100}, a transition from free soluble diblocks to soluble nanoparticles was observed after ca. 3–4 days as an increase in the total scattering intensity. This was accompanied by the disappearance of the fast relaxation mode characteristic of free polyelectrolyte chains. After 7 days the scattering intensity leveled off and remained constant thereafter. Dynamic light scattering revealed two populations (intensity distributions) with diameters 25 and 150 nm, but only the former was detectable in the estimated number distributions. It thus seems this combination of chain lengths provides core-corona nanoparticles. The length of the G-block (m = 40) is well above the DP needed for strong binding of calcium ions[5,23] whereas the dextran block (n = 100) did not reach a volume large enough to prevent self-assembly. The lower limit with respect to the chain length of the dextran block remains to be identified. Lowering the G-block length to 11, which is closer to the critical length for strong calcium binding and chain dimerization, and which has a chain size appreciably smaller than the dextran did not provide well defined nanoparticles, but rather loose aggregates.

8. Conclusions

Early research on the nature of alginates provided methods for excising and purifying the principal block types of alginates. More recent research has demonstrated that the Ca-reactive G-blocks can modify both gelation kinetics, equilibrium elasticity, and syneresis in alginate gels. They can further modify transport properties of mucus. G-blocks can further be terminally conjugated to other blocks to obtain a new generation of Ca-sensitive diblock polysaccharides which instead of precipitation or forming hydrogels instead form well-defined nanoparticles by spontaneous self-assembly without the need for mechanical treatments or complex mixing methods. To this end the diblock G_m-*b*-Dex_n has been briefly investigated. It seems reasonable to assume that the mode of self-assembly of G_{40}-*b*-Dex_{100} with Ca^{++} corresponds to a core consisting of G-blocks crosslinked with calcium ions according to the egg-box-model whereas the dextran block for an outer corona endowed with stabilizing properties. Future research will focus on a wider range of block sizes, different rates and modes of calcium delivery, and investigation of other cations known to bind strongly to alginate G-blocks such as strontium and barium ions. Due to the nanometer size of the particles combined with the cation-binding properties of the G-blocks, these systems may be attractive in biomedical areas related to alginate-binding cations, for example, in transport and delivery of radionuclides.

Conflict of Interest

The authors declare no conflict of interest.

Data Availability Statement

Data sharing not applicable – no new data generated.

Keywords

alginate, diblocks, G-blocks, nanoparticles, self-assembly

Received: February 3, 2022
Revised: April 24, 2022

[1] O. Smidsrød, *Faraday Discuss. Chem. Soc.* **1974**, *57*, 263.
[2] K. I. Draget, S. T. Moe, G. Skjåk-Bræk, O. Smidsrød, in *Food Polysaccharides and Their Applications*, 2nd ed. (Eds: A.M. Stephen, G.O. Phillips, P.A. Williams), CRC Press, Boca Raton **2006**, p. 289.
[3] B. Larsen, T. Painter, A. Haug, O. Smidsrød, *Acta Chem. Scand.* **1969**, *23*, 355.
[4] C. Taylor, K. I. Draget, O. A. Smidsrød, 8,884,1279 **2008**.
[5] R. Kohn, B. Larsen, *Acta Chem. Scand.* **1972**, *26*, 2455.
[6] C. Campa, A. Oust, G. Skjak-Braek, B. S. Paulsen, S. Paoletti, B. E. Christensen, S. Ballance, *J. Chromatogr. A* **2004**, *1026*, 271.
[7] A. Haug, O. Smidsrød, *Chem. Soc. Spec. Publ.* **1968**, *23*, 273.
[8] S. Holtan, Q. Zhang, W. I. Strand, G. Skjåk-Bræk, *Biomacromolecules* **2006**, *7*, 2108.
[9] O. Smidsrød, B. Larsen, T. Painter, A. Haug, *Acta Chem. Scand.* **1969**, *23*, 1573.
[10] O. Smidsrød, A. Haug, B. Larsen, *Acta Chem. Scand.* **1966**, *20*, 1026.
[11] O. A. Aarstad, A. Tøndervik, H. Sletta, G. Skjåk-Bræk, *Biomacromolecules* **2012**, *13*, 106.
[12] A. Solberg, I. V. Mo, M. Ø. Dalheim, F. L. Aachmann, C. Schatz, B. E. Christensen, *Polym. Chem.* **2021**, *12*, 5412.
[13] O. Smidsrød, A. Haug, *Acta Chem. Scand.* **1972**, *26*, 2063.
[14] P. Sikorski, F. Mo, G. Skjåk-Bræk, B. T. Stokke, *Biomacromolecules* **2007**, *8*, 2098.
[15] G. T. Grant, E. R. Morris, D. A. Rees, P. J. C. Smith, D. Thom, *FEBS Lett.* **1973**, *32*, 195.
[16] I. Donati, P. Paoletti, *Alginates: Biology and Applications*, Springer-Verlag, Berlin, Heidelberg **2009**.
[17] B. T. Stokke, K. I. Draget, O. Smidsrød, Y. Yuguchi, H. Urakawa, K. Kajiwara, *Macromolecules* **2000**, *33*, 1853.
[18] M. K. Simensen, K. I. Draget, E. Onsøyen, O. Smidsrød, WO 98/02488 **1998**.
[19] K. I. Draget, O. Smidsrød, in *Gums and Stabilisers for the Food Industry*, vol. *13* (Eds: P.A. Williams, G.O. Phillips), RSC Publishing **2006**, p. 227.
[20] C. T. Nordgard, K. I. Draget, *Biomacromolecules* **2011**, *12*, 3084.
[21] C. T. Nordgard, U. Nonstad, M. O. Olderoy, T. Espevik, K. I. Draget, *Biomacromolecules* **2014**, *15*, 2294.
[22] A. Solberg, I. V. Mo, L. A. Omtvedt, B. L. Strand, F. L. Aachmann, C. Schatz, B. E. Christensen, *Carbohydr. Polym.* **2022**, 278.
[23] K. A. Bowman, O. A. Aarstad, M. Nakamura, B. T. Stokke, G. Skjak-Braek, A. N. Round, *Carbohydr. Polym.* **2016**, *148*, 52.